Global Translation Preferred Active Contour

LI Xiao-mao[1),2)], TANG Yan-dong[1)], ZHU Lin-lin[1),2)]

[1)] (*State Key Laboratory of Robotics, Shenyang Institute of Automation, Chinese Academy of Sciences, Shenyang* 110016)

[2)] (*Graduate School of the Chinese Academy of Sciences, Beijing* 100039)

Abstract　Global translation preferred active contour is much more suitable for object tracking. The prior information of active contour with global translation preference can be interpreted as the velocity field along the evolving contour with equivalency preference. According to this, a simple gradient flow which preferes global translation is acquired by defining a new inner product on the set of perturbations of a curve. The new inner product is obtained by adding the variance of the perturbation of a curve to the inner product relative to the $\boldsymbol{H}^0$ active contour. The active contour relative to the new inner product is called variance active contour. In contrast to $\boldsymbol{H}^1$ active contour generated by convolution of $\boldsymbol{H}^0$ active contour and certain kernel functional, variance active contour needs no convolution and is a weighting sum of $\boldsymbol{H}^0$ active contour and corresponding average gradient flow. Thus, variance active contour can be implemented much faster and easier than $\boldsymbol{H}^1$ active contour. We also compared $\boldsymbol{H}^0$, $\boldsymbol{H}^1$ and variance active contours in space and frequency domains.

Keywords　variance active contour, Sobolev active contours, inner products, gradient flows, Gâteaux derivative

中图法分类号:TP391.41　　**文献标识码**:A　　**文章编号**:1006-8961(2008)08-1588-06

全局平移优先主动轮廓

李小毛[1),2)]　唐延东[1)]　朱琳琳[1),2)]

[1)](中国科学院沈阳自动化研究所机器人学国家重点实验室,沈阳　110016)

[2)](中国科学院研究生院,北京　100039)

摘　要　具有全局平移优先属性的主动轮廓更适于目标跟踪。演化轮廓具有的全局平移优先性可以理解为沿轮廓的速度场具有相等的倾向。根据此思想,通过定义在曲线扰动集合上的新内积空间导出了一种简单,具有平移优先的梯度流。新的内积空间由于是通过向 $\boldsymbol{H}^0$ 主动轮廓对应的内积空间引入曲线扰动的方差获得,所以此主动轮廓称为方差主动轮廓。方差主动轮廓是将 $\boldsymbol{H}^0$ 主动轮廓与其对应的平均梯度流通过加权求和获得,而 $\boldsymbol{H}^1$ 主动轮廓则是通过 $\boldsymbol{H}^0$ 主动轮廓与特定类型的核函数进行卷积得到。因此方差主动轮廓实现时更简单和快速。最后给出了 $\boldsymbol{H}^0$,$\boldsymbol{H}^1$ 和方差主动轮廓在频域与时域的分析。

关键词　方差主动轮廓　索伯列夫主动轮廓　内积　梯度流　加特微分

1　Introduction

Active contour model, also known as snake model, was pioneered in 1987 by Kass *et al* in [1] for image segmentation via driving an initial contour toward a desired object edge with a PDE deduced by minimizing an energy functional. But it has many limitations. For example, this model can hardly be applied to images with topological change. It is sensitive to initial contour placement, and strongly depends on curve parameterization. In 1993, geodesic

基金项目:机器人学国家重点实验室开放课题基金项目(07A1210101)

收稿日期:2008-04-10;**改回日期**:2008-04-20

第一作者简介:李小毛(1981～　),男。现为中国科学院沈阳自动化研究所及中国科学院研究生院硕博研究生。2003 年于沈阳理工大学获测控技术与仪器专业工学学士学位。主要研究方向为基于变分和偏微分方程的图像处理、自动目标识别及跟踪。

E-mail: lixiaomaosia@gmail.com

active contour[2], formulated as a weighting Euclidean arc length using a edge-stopped potential functional, was proposed by Casselles *et al* in a level set framework[3]. Those models mentioned above are edge-based[2,4]. In most cases, they are less robust for image segmentation than region-based active contour models[5~7] which utilize certain image global region statistical information, partitioning off a given image into statistically distinct regions. The Mumford-Shah (M-S)[8] model can be considered as a whole image segmentation functional framework for edge and region based active contour models. Active contours utilize the edge and region information in a whole variation of framework presented in [9].

In order to obtain desirable segmentation results, an important strategy for active contours research is combining certain prior knowledge with object information to deal with images with insufficient information. Some paradigms making use of prior shape and topology information can be found in [10 ~ 14]. For more recent developments about active contours, we refer the readers to [15]、[16].

In order to entitle curve evolution to certain desirable features, prior information on the deformation field of evolving contours can also be used. Clearly, the gradient flow driving curve evolution derived by minimizing its corresponding energy functional is directly relative to the choice of the inner product on the deformation field defined on a manifold of curves. Thus, a prior information on the deformation field can be embodied directly by the choice of the inner product[17]. However, before the appearances of [17]、[18], the authors focused on energy functional building, while they ignored the relation between gradient flows and choices of inner products completely and considered that the deformation field is ruled by the L^2-type inner product called $\boldsymbol{H}^0$ active contour in [18]. Due to the arbitrary evolution of $\boldsymbol{H}^0$ active contour which results in many undesirable features[18], Sundaramoorthi *et al* used the $\boldsymbol{H}^1$-type inner product to define the gradient flow for active contour called $\boldsymbol{H}^1$ active contour[18] which has many advantages over $\boldsymbol{H}^0$ active contour. For example, favorable global translations, better regularity properties and desirable ability of coarse to fine motion, are more suitable for image segmentation and object tracking.

In this paper, a new active contour called variance active contour is proposed, favoring global translation. However, $\boldsymbol{H}^1$ active contour is a convolution of $\boldsymbol{H}^0$ active contour and a kernel functional, while variance active contour is a simple weighting sum of $\boldsymbol{H}^0$ active contour and corresponding average gradient flow, derived by solving a simple algebra equation. In contrast to $\boldsymbol{H}^1$ active contour, variance active contour can be realized exactly by using level set methods without polygon extraction and canbe implemented easily and fast.

2　$\boldsymbol{H}^1$ active contour

Let M denote the set of smooth embedded curves in $\mathbf{R}^n$, which is a differentiable manifold. For $C \in \boldsymbol{M}$, the tangent space of $\boldsymbol{M}$ at C denotes by $\boldsymbol{T}_C\boldsymbol{M}$, which can be seen as the deformation space. Given energy functional $E(C)$, the process of computation its Gâteaux derivative $\delta E(C,\boldsymbol{\eta})$ can be expressed as:

$$\delta E(C,\boldsymbol{\eta}) \overset{\text{def}}{=} \lim_{\varepsilon \to 0} \frac{E(C+\varepsilon\boldsymbol{\eta}) - E(C)}{\varepsilon} \tag{1}$$

In order to get the gradient flow of $E(C)$, we must model the deformation space $\boldsymbol{T}_C\boldsymbol{M}$ as an inner product space denoted by $(\boldsymbol{F}, \langle,\rangle_{\boldsymbol{F}})$. The gradient flow $\nabla_{\boldsymbol{F}}E(C) \in \boldsymbol{T}_C\boldsymbol{M}$, which is relative to the defined inner product exists when it satisfies the following conditions.

$$\forall \boldsymbol{\eta} \in \boldsymbol{T}_C\boldsymbol{M}\quad \delta E(C,\boldsymbol{\eta}) = \langle \nabla_{\boldsymbol{F}}E, \boldsymbol{\eta}\rangle_{\boldsymbol{F}}, \nabla_{\boldsymbol{F}}E \text{ is unique} \tag{2}$$

The inner products for $\boldsymbol{H}^0$ and $\boldsymbol{H}^1$ active contours are defined as following.

$$\langle h,k\rangle_{\boldsymbol{H}^0} := \frac{1}{L}\int_0^L h(s)\cdot k(s)\,\mathrm{d}s$$

$$\langle h,k\rangle_{\boldsymbol{H}^1} := \langle h,k\rangle_{\boldsymbol{H}^0} + \lambda L^2 \langle h',k'\rangle_{\boldsymbol{H}^0} \tag{3}$$

where $\lambda \geqslant 0$ is a weighting coefficient, L is the length of C, $h(s)$ and $k(s) \in \boldsymbol{T}_C\boldsymbol{M}$ parameterized by the arclength of curve and the derivatives on $h(s)$ and $k(s)$ are with respect to arclength. At last, the relation between gradient flows for $\boldsymbol{H}^0$ and $\boldsymbol{H}^1$ active contours can be established by solving an ODE derived via relations between $\boldsymbol{H}^0$ and $\boldsymbol{H}^1$ inner products defined above.

$$\nabla_{H^1} E = \nabla_{H^0} E * K_\lambda$$

$$K_\lambda(s) = \frac{\cosh\left(\frac{s - L/2}{\sqrt{\lambda} L}\right)}{2L\sqrt{\lambda}\sinh\left(\frac{1}{2\sqrt{\lambda}}\right)} \tag{4}$$

3 Variance active contour

3.1 New inner product of variance active contour

The prior information of active contour with global translation preference can also be interpreted as the velocity field along the evolving contour with equivalency preference (see Fig. 1). When the evolving curve C has a globally pure translation $\boldsymbol{T}(s) = \Delta C(s)$, the variance of velocity field along $\boldsymbol{C}$ is zero. Base on this fact, we define the following inner products to entitle active contour to global translation preference.

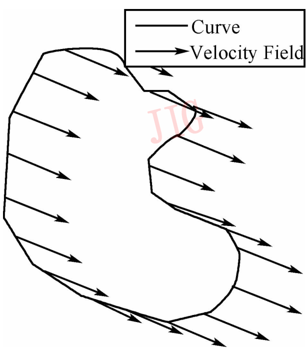

Fig. 1 Equal velocities along the evolving curve

$$\langle h, k\rangle_{H^V} := \langle h, k\rangle_{H^0} + \lambda\langle h - \bar{h}, k - \bar{k}\rangle_{H^0} \tag{5}$$

$$\langle h, k\rangle_{\tilde{H}^V} := \bar{h}\cdot\bar{k} + \lambda\langle h - \bar{h}, k - \bar{k}\rangle_{H^0} \tag{6}$$

$$\bar{h} = \frac{1}{L}\int_0^L h(s)\,\mathrm{d}s; \quad \bar{k} = \frac{1}{L}\int_0^L k(s)\,\mathrm{d}s \tag{7}$$

It is easy to verify that the above two definition are inner products. We can see that the smoother the deformation field is along the evolving curve, the smaller the norm derived by inner products defined in equations (5) and (6) is. By this feature, it can be induced that variance active contour favors global translation, but not restrict to this motion.

3.2 Gradients of variance active contour

In this subsection, we deduce the relationships between variance and $\boldsymbol{H}^0$ active contours. We can get the following equation via equations (2) and (5).

$$\langle \boldsymbol{\eta}, \nabla_{H^V} E\rangle_{H^V} = \langle \boldsymbol{\eta}, \nabla_{H^V} E + \lambda(\nabla_{H^V} E - \overline{\nabla_{H^V} E})\rangle_{H^0} \tag{8}$$

If a gradient corresponding to a given inner product exists, it is unique. Thus, we can get the following equation.

$$\nabla_{H^V} E + \lambda(\nabla_{H^V} E - \overline{\nabla_{H^V} E}) = \nabla_{H^0} E \tag{9}$$

For $\overline{\nabla_{H^V} E} = \overline{\nabla_{H^0} E}$, the relation between the two gradients can be written as.

$$\nabla_{H^V} E = \frac{\nabla_{H^0} E}{1 + \lambda} + \lambda\frac{\overline{\nabla_{H^0} E}}{1 + \lambda} \tag{10}$$

We can get the $\tilde{\boldsymbol{H}}^V$ gradient using the similar approach, obtaining that $\tilde{\boldsymbol{H}}^V$ and $\boldsymbol{H}^V$ gradients are the same. As $\lambda \to \infty$, the $\boldsymbol{H}^V$ gradient flow holds globally pure translation equal to the average $\boldsymbol{H}^0$ gradient flow, while it degenerates into the $\boldsymbol{H}^0$ gradient flow as $\lambda \to 0$. Although the variance and the $\boldsymbol{H}^1$ active contours both favor global translation, the gradient flow of the variance active contour is a simple weighting sum of $\boldsymbol{H}^0$ active contour and corresponding average gradient flow and the gradient flow of $\boldsymbol{H}^1$ is a convolution of $\boldsymbol{H}^0$ active contour and a kernel function.

4 Comparison of Variance, H^0 and H^1

It is easy to see that the norm of the second term relative to inner products for $\boldsymbol{H}^1$ active contour also becomes zero, when the evolving curve only has a globally pure translation. Thus, $\boldsymbol{H}^1$ active contour also prefers global translation. $\boldsymbol{H}^1$ active contour possesses other favorable properties compared with variance active contour, such as, from coarse to fine motion, much more regularity, but costs are also high, for example, the convolution computation and polygon extraction in the level set framework. By equation (2), we get the following relation.

$$\langle \nabla_{H^V} E, \boldsymbol{\eta}\rangle_{H^V} = \langle \nabla_{H^0} E, \boldsymbol{\eta}\rangle_{H^0} \text{ For all } \boldsymbol{\eta} \in \boldsymbol{T}_C\boldsymbol{M} \tag{11}$$

Using Parseval's Theorem, we get that.

$$\widehat{\nabla_{H^V} E}(0) = \widehat{\nabla_{H^0} E}(0)$$

$$\widehat{\nabla_{H^V} E}(l) = \frac{\widehat{\nabla_{H^0} E}(l)}{1+\lambda} \quad l \in \boldsymbol{Z} \setminus \{0\} \tag{12}$$

where ^ represents the Fourier transform. The Fourier series for $\boldsymbol{H}^1$ active contour can be written as[18].

$$\widehat{\nabla_{H^1} E}(0) = \widehat{\nabla_{H^0} E}(0)$$

$$\widehat{\nabla_{H^1} E}(l) = \frac{\widehat{\nabla_{H^0} E}(l)}{1+\lambda(2\pi l)^2} \quad l \in \boldsymbol{Z} \setminus \{0\} \tag{13}$$

From equations (12) and (13), we find that, for the zero frequency components of $\boldsymbol{H}^1$ and $\boldsymbol{H}^V$ active contours play a more important role than $\boldsymbol{H}^0$ active contour, they have global translation preference. However, except the zero frequency component, the decay coefficients of $\boldsymbol{H}^1$ active contour fourier series are relative to frequency, while the ones of variance active contour are not and only relative to λ. This can be interpreted as that we only consider the average perturbation of curves corresponding to the zero frequency. However, the variance active contour possesses better regularity and global property than $\boldsymbol{H}^0$ active contour and has simpler expression than $\boldsymbol{H}^1$ active contour inducing fast and easy realization.

5 Numerical experiments

In this section we give some experiments to demonstrate the characteristics of variance active contour. The weighting coefficient λ in equation (5) as well as equation (3) is chosen as 20 in the subsequent numerical experiments, although higher λ entitles them to better global translation preference and produce similar results. The following experiments were realized based on the *C-V* model[5].

In Fig. 2, we compare the segmenting results of a noisy square image using the usual $\boldsymbol{H}^0$ and $\boldsymbol{H}^V$ active contours respectively. The initial contours of the methods are the same (see Fig. 2 (a)). It shows that $\boldsymbol{H}^V$ active contour with global translation possesses favorable regularity properties, while the final configuration of $\boldsymbol{H}^0$ is undesirable due to arbitrary distribution of velocities along evolving contours.

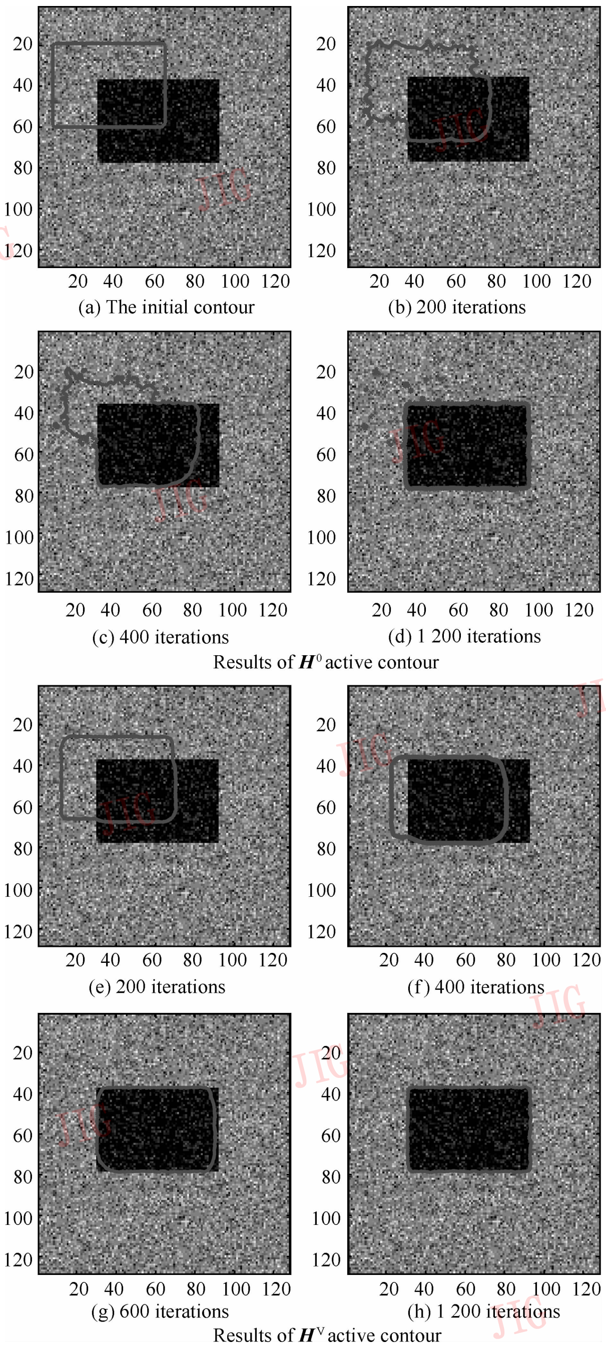

Fig. 2 Segmentation results for a nosiy square image using $\boldsymbol{H}^0$ and $\boldsymbol{H}^V$ active contours respectively

Fig. 3 shows the velocity distribution of the 400th iteration of the $\boldsymbol{H}^V$ active contour in Fig. 2 for $\boldsymbol{H}^0$ and $\boldsymbol{H}^V$ active contours respectively. From it we can obtain that the velocity of $\boldsymbol{H}^V$ active contour is uniformly distributed, while the one of $\boldsymbol{H}^0$ active contour seems noisy. Thus, Fig. 3 can well interpret the results of Fig. 2.

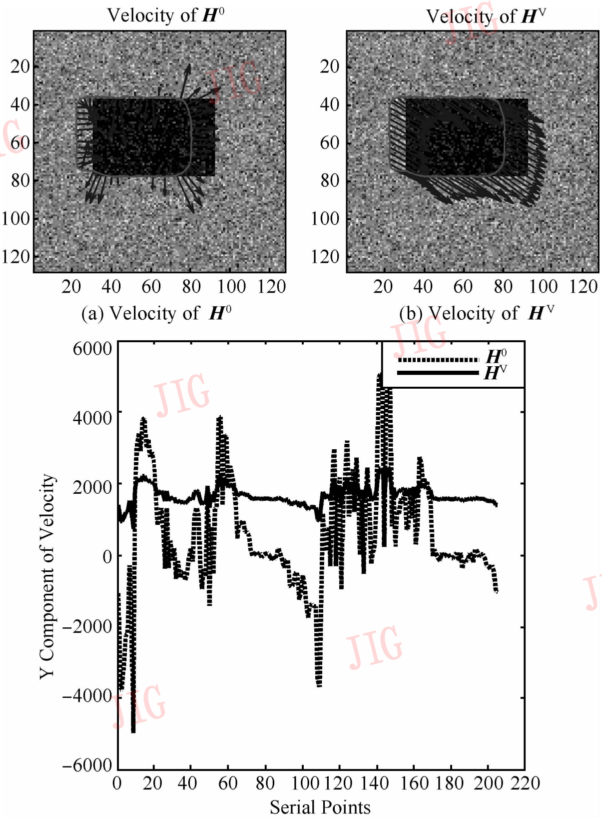

(a) Velocity of $\boldsymbol{H}^0$ (b) Velocity of $\boldsymbol{H}^V$

(c) Y component of unwraped velocity along evolving contours of $\boldsymbol{H}^0$ and $\boldsymbol{H}^V$ active contours

Fig. 3 Velocity distribution of the 400th iteration of the $\boldsymbol{H}^V$ active contour in Fig. 2 for $\boldsymbol{H}^0$ and $\boldsymbol{H}^V$ active contours

Fig. 4 shows some snapshots of the evolution of a circular object segmentation, using $\boldsymbol{H}^0$, $\boldsymbol{H}^1$ and $\boldsymbol{H}^V$ active contours respectively. The initial contour is a circle with a translation from the segment object. We can see that $\boldsymbol{H}^0$ active contour deforms the initial contour arbitrarily to reduce energy giving rise to many unnecessary and unlikely shapes, while $\boldsymbol{H}^1$ and $\boldsymbol{H}^V$ active contours with global translation preference favor preserving the initial shape.

Tab. 1 gives the comparisons of Fig. 4 among $\boldsymbol{H}^0$, $\boldsymbol{H}^1$ and $\boldsymbol{H}^V$ active contours. From Tab. 1, we can deduce that the iterations of $\boldsymbol{H}^V$ active contour are less than $\boldsymbol{H}^0$ but more than $\boldsymbol{H}^1$ and the consuming time of $\boldsymbol{H}^V$ active contour is the least. This can be interpreted that $\boldsymbol{H}^V$ active contour have less global translation than $\boldsymbol{H}^1$ with the same λ, while more than $\boldsymbol{H}^0$ active contour and the cost time for each iteration of $\boldsymbol{H}^1$, $\boldsymbol{H}^V$, and $\boldsymbol{H}^0$ active contours is in a decreasing rank.

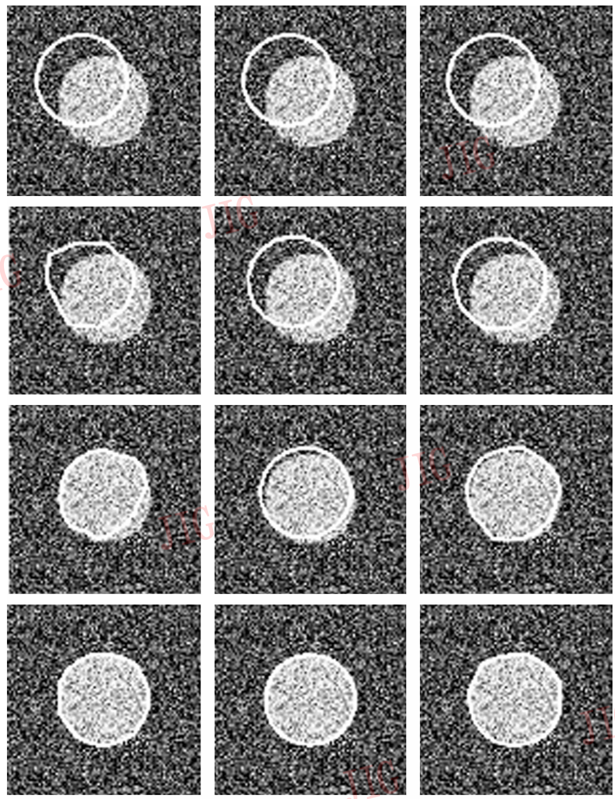

(a) $\boldsymbol{H}^0$ (b) $\boldsymbol{H}^1$ (c) $\boldsymbol{H}^V$

Fig. 4 From left to right, snapshots of a noisy circular object segmentation using region-based energy by $\boldsymbol{H}^0$ (with a regularization term), $\boldsymbol{H}^1$ and $\boldsymbol{H}^V$ active contours

Tab. 1 Comparison of Fig. 4 among $\boldsymbol{H}^0$, $\boldsymbol{H}^1$ and $\boldsymbol{H}^V$

Methods	Iterations	Time(s)
$\boldsymbol{H}^0$	77	2.13
$\boldsymbol{H}^1$	13	0.6
$\boldsymbol{H}^V$	17	0.45

6 Conclusion

A new inner product was defined based on prior information that is prior to globally pure translation for curve evolution. Active contour corresponding to the new inner product is named as variance active contour. Then, the gradient flow of variance active contour was deduced. The analysis and the comparisons were given among $\boldsymbol{H}^0$, $\boldsymbol{H}^1$ and variance active contours. By analysis, the prior information for variance and $\boldsymbol{H}^1$ active contours can be considered that the deformation fields along evolving curves are uniform distribution and smoothness respectively. Variance active contour can also be considered as a transition between $\boldsymbol{H}^0$ and $\boldsymbol{H}^1$ active contours, because variance active contour has more favorable features than $\boldsymbol{H}^0$ active contour, but less than $\boldsymbol{H}^1$ active contour. In contrast to $\boldsymbol{H}^1$ active contour, variance active contour can be implemented without polygon extraction using level set method and can be implemented fast and easily.

Acknowledgement We thank Prof. Dr. Hongyi Li for his valuable suggestion on the paper.

References

1 Kass M, Witkin A, Terzopoulos D. Snakes: active contour models [J]. International Journal of Computer Vision, 1988, **1**(4): 321～331.

2 Casselles V, Catte F, Coll T, *et al*. A geometric model for active contours[J]. Numerische Mathematik, 2005, **66**(1): 1～31.

3 Osher S, Sethian J A. Fronts propagating with curvature dependent speed: algorithms based on hamilton-jacobi formulations[J]. Journal of Computational Physics, 1988, **79**(1):12～49.

4 Kichenassamy S, Kumar A, Olver P, *et al*. Gradient flows and geometric active contour models[A]. In: Proceedings of IEEE Fifth International Conference on Computer Vision[C]. Boston, MA, USA. 1995:810～815.

5 Chan T, Vese L A. Active contours without edges[J]. IEEE Transactions on Image Processing, 2001, **10**(2):266～277.

6 Yezzi A, Tsai A, Willsky A S. A fully global approach to image segmentation via coupled curve evolution equations[J]. Journal of Visual Communication and Image Representation, 2002, **13**(1):195～216.

7 Junmo K, Fisher J W, Yezzi A, *et al*. A nonparametric statistical method for image segmentation using information theory and curve evolution[J]. IEEE Transactions on Image Processing, 2005, **14**(10):1486～1502.

8 Mumford D, Shah J. Optimal approximation by piecewise smooth functions and associated variational problem[J]. Communications on Pure and Applied Mathematics, 1989, **42**(5):577～685.

9 Paragios N, Deriche R. Geodesic Active regions: a new paradigm to deal with frame partition problems in computer vision[J]. Journal of Visual Communication and Image Representation, 2002, **13**(1):249～268.

10 Leventon M E, Grimson W E L, Faugeras O. Statistical shape influence in geodesic active contours[A]. In: Proceedings of IEEE Conference on Computer Vision and Pattern Recognition [C]. Hilton Head, SC, USA. 2000:1316～1323.

11 Chen Y, Tagare H D, Thiruvenkadam S, *et al*. Using prior shapes in geometric active contours in a variational framework [J]. International Journal of Computer Vision, 2002, **50**(3):315～328.

12 Cremers D. Dynamical statistical shape priors for level set based tracking[J]. IEEE Transactions on Pattern Analysis and Machine Intelligence, 2006, **28**(8):1262～1273.

13 Han X, Xu C, Prince J L. A topology preserving level set method for geometric deformable models[J]. IEEE Transactions on Pattern Analysis and Machine Intelligence, 2003, **25**(6):755～768.

14 Sundaramoorthi G, Yezzi A. More than topology preserving flows for active contours and polygons[A]. In: Proceedings of IEEE Tenth International Conference on Computer Vision[C]. Beijing, China, 2005:1276～1283.

15 Cremers D, Rousson M, Deriche R. A review of statistical approaches to level set segmentation: integrating color, texture, motion and shape[J]. International Journal of Computer Vision, 2007, **72**(2):195～215.

16 Chan T, Sandberg B, Moelich M. Some Recent Developments in Variational Image Segmentation[R]. cam06-52, University of California, Los Angeles, CA, USA,2006:1～36.

17 Charpiat Maurel P, Pons J P, Keriven R, *et al*. Generalized gradients: priors on minimization flows[J]. International Journal of Computer Vision, 2007, **73**(3):325～344.

18 Sundaramoorthi G, Yezzi A, Mennucci A. Sobolev active contours [A]. In: Proceedings of Conference on Variational, Geometric, and Level Set Methods in Computer Vision[C]. Beijing, China, 2005:109～120.